Generalized Belief Propagation Algorithm for the Capacity of Multi-Dimensional Run-Length Limited Constraints

Giovanni Sabato
PARALLEL Informatik AG
CH-6005 Luzern
Switzerland
giovanni.sabato@parallel.ch

Mehdi Molkaraie
Dept. Inform. Techn. & Electr. Eng.
ETH Zurich
CH-8092 Zürich, Switzerland
mehdi.molkaraie@isi.ee.ethz.ch

***Abstract*— The performance of the generalized belief propagation algorithm for computing the noiseless capacity of finite-sized two-dimensional and three-dimensional run-length limited constraints is investigated. For each constraint, a method is proposed to choose a set of clusters. Simulation results for different sizes of channels with different constraints are reported. Convergence to the Shannon capacity is also discussed.**

I. Introduction

Run-length limited (RLL) constraints are widely used in magnetic and optical recording systems. Such constraints reduce the effect of inter-symbol interference and help in timing control. In track-oriented storage systems constraints are defined in one dimension.

We say a binary one-dimensional (1-D) sequence satisfies the (d, k)-RLL constraint if the runs of 0's have length at most k and the runs of 0's between successive 1's have length at least d. We suppose that $0 \leq d < k \leq \infty$.

The *Shannon capacity* of a 1-D (d, k)-RLL constraint is defined as

$$C_{1D}^{(d,k)} \triangleq \lim_{m \to \infty} \frac{\log_2 Z(m)}{m}, \tag{1}$$

where $Z(m)$ denotes the number of binary 1-D sequences of length m that satisfy the (d, k)-RLL constraint, see [10].

With recent developments in page-oriented storage systems, such as holographic data storage, two-dimensional (2-D) constraints have become more of interest [12]. In these systems, data is organized on a surface and constraints are defined in two dimensions.

A 2-D binary array satisfies the (d_1, k_1, d_2, k_2)-RLL constraint if it satisfies a (d_1, k_1)-RLL constraint horizontally and a (d_2, k_2)-RLL constraint vertically. If a 2-D binary array satisfies a 1-D (d, k)-RLL constraint both horizontally and vertically, we simply say that it satisfies a 2-D (d, k)-RLL constraint.

Example 1 (2-D $(2, \infty)$-RLL constraint)
The 2-D $(2, \infty)$-RLL constraint is satisfied in the following 2-D binary array segment. In words, in every row and every column of the array there are at least two 0's between successive 1's; but the runs of 0's can be of any length (however, 1's can be diagonally adjacent).

$$\begin{array}{c}
\ldots 0100100001001000100000100010 \ldots \\
\ldots 1000010000100010000100000100 \ldots \\
\ldots 0001000010000001000000010001 \ldots \\
\ldots 0100100100010000001000100000 \ldots
\end{array}$$

The Shannon capacity of a 2-D (d_1, k_1, d_2, k_2)-RLL constraint is defined as

$$C_{2D}^{(d_1,k_1,d_2,k_2)} \triangleq \lim_{m,n \to \infty} \frac{\log_2 Z(m, n)}{mn}, \tag{2}$$

where $Z(m, n)$ denotes the number of 2-D binary arrays of size $m \times n$ that satisfy the (d_1, k_1, d_2, k_2)-RLL constraint.

Similarly, the Shannon capacity can be defined for higher dimensional constrained channels. For example, the Shannon capacity in three dimensions $C_{3D}^{(d_1,k_1,d_2,k_2,d_3,k_3)}$ depends on $Z(m, n, q)$, the number of three-dimensional (3-D) binary arrays of size $m \times n \times q$ satisfying a $(d_1, k_1, d_2, k_2, d_3, k_3)$-RLL constraint.

The capacity C is an important quantity that provides an upper bound to the information rate of any encoder that maps arbitrary binary input into binary data that satisfies certain constraints.

There are a number of techniques to compute the 1-D Shannon capacity (for example combinatorial or algebraic approaches) [3]. In contrast to the 1-D capacity, except for a few cases, exact values of two and higher dimensional (positive) capacities are not known, see [1], [2], [4], [13], [14].

In this paper, we use ideas from statistical mechanics and generalized belief propagation (GBP) to approximate the noiseless capacity of 2-D and 3-D RLL constrained channels. Our main motivations were the successful application of GBP for the information rate of 2-D finite-state channels with memory in [11] and tree-based Gibbs sampling for the noiseless capacity of 2-D constrained channels in [7].

II. Problem Set-up

Consider a set $\{X_1, X_2, \ldots, X_N\}$ of discrete random variables taking values in finite sets $\mathcal{X}_1, \mathcal{X}_2, \ldots, \mathcal{X}_N$. Let $\mathcal{X}$ be the Cartesian product $\mathcal{X} = \mathcal{X}_1 \times \mathcal{X}_2 \ldots \times \mathcal{X}_N$. Let $\mathbf{x}$ stand for $\{x_1, x_2, \ldots, x_N\}$ where x_i represents the possible realization of X_i.

Suppose $f(\mathbf{x})$ is an indicator function as follows,

$$f(\mathbf{x}) = \begin{cases} 1, & \text{if } \mathbf{x} \text{ satisfies the RLL constraint,} \\ 0, & \text{otherwise.} \end{cases} \tag{3}$$

We are interested in computing Z defined as (also known as the *partition function*, see Section III)

$$Z \triangleq \sum_{\mathbf{x} \in \mathcal{X}} f(\mathbf{x}). \tag{4}$$

With the above assumptions, the sum (4) counts the number of sequences that satisfy a given RLL constraint. Therefore computing the capacity of RLL constraints is closely related to computing the sum in (4).

Since RLL constraints impose restrictions on the values of variables that can be verified locally, we can assume that $f(\mathbf{x})$ factors into a product of non-negative local kernels as

$$f(\mathbf{x}) = \prod_a f_a(\mathbf{x}_a), \tag{5}$$

where the kernel $f_a(\mathbf{x}_a)$ has $\mathbf{x}_a$ some subset of $\mathbf{x}$ as arguments.

The factorization in (5) can be represented with a graphical model. In this paper, we focus on graphical models defined in terms of *(Forney-style) factor graphs.* If the factorization (5) yields a cycle-free factor graph, the sum in (4) can be computed efficiently by the sum-product message passing algorithm [6].

However, for the examples we study in this paper, factor graphs have (many short) cycles, see Fig. 1. In such cases computing Z, as expressed in (4), needs a sum with an exponential number of terms. Therefore we are interested in applying approximate methods.

Due to the presence of many short cycles in factor graph representation of 2-D and 3-D RLL constraints, loopy belief propagation often fails to converge. As a result, we apply GBP and ideas from statistical mechanics to estimate Z which leads to estimating the capacity of RLL constraints.

III. GBP AND THE REGION GRAPH METHOD

In statistical physics, the quantity Z in (4) is known as the partition function and the *Helmholtz free energy* is defined as

$$F_H \triangleq -\ln(Z). \tag{6}$$

The partition function and the Helmholtz free energy are important quantities in statistical physics since they carry information about all thermodynamic properties of a system.

A number of techniques have been developed in statistical physics to approximate the free energy. The method we apply in this paper is known as the region-based free energy approximation, in particular we use the cluster variation method to select a valid set of regions and counting numbers, see [16].

We start by introducing the region graph representing our problem. Such a region graph will provide a graphical framework for GBP. For each RLL constraint, the size of the basic region is chosen based on the constraint parameters. For a 2-D (d_1, k_1, d_2, k_2)-RLL constraint with finite k_1 and k_2, the width and the height of the basic region is chosen as

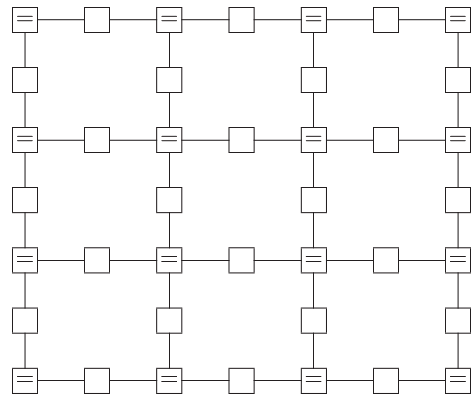

Fig. 1. Forney-style factor graph for a 2-D $(1,\infty)$-RLL constraint.

$$\begin{aligned} W_R &= k_1 + 1 \\ H_R &= k_2 + 1, \end{aligned}$$

and for the infinite case, the size is chosen as $d+1$, see [9].

Such a choice for the basic regions seems plausible since the validity of a given array can be determined by verifying the constraints in each region and sliding it along the rows and along the columns of the array. See the region graph for a 2-D $(1,\infty)$-RLL constraint in Section III-A.

After forming the region graph using the cluster variation method, we perform GBP on this graph by sending messages between the regions while performing exact computations inside each region.

We will need the region-based free energy to estimate the number of arrays that satisfy a given constraint. Therefore, we first operate GBP on the corresponding region graph until convergence and use the obtained region beliefs $b_R(\mathbf{x}_R)$ to compute the region-based free energy $\hat{F}_H$ (as an estimate of F_H) as

$$\begin{aligned} \hat{F}_H &= \min_{\{b_R\}} F_{\mathcal{R}}(\{b_R(\mathbf{x}_R)\}) \\ &= \sum_{R \in \mathcal{R}} c_R \sum_{\mathbf{x}_R} b_R(\mathbf{x}_R) \Big(\ln b_R(\mathbf{x}_R) - \ln \prod_a f_a(\mathbf{x}_a) \Big) \end{aligned} \tag{7}$$

Here $\mathbf{x}_R$ stands for the set of variables in region R, the set of all regions is denoted by $\mathcal{R}$, and c_R is the counting number.

Secondly, we use $\hat{F}_H$ to estimate the finite-sized capacity of the RLL constraint. Finally, we demonstrate how the capacity converges (to the Shannon capacity, see Fig. 4) by increasing the size of the channel.

A. A Region Graph for a 2-D $(1,\infty)$-RLL Constraint

Consider a grid of $N = m \times m$ binary random variables. The 2-D $(1,\infty)$-RLL constraint is satisfied if no two (horizontally or vertically) adjacent variables have both the value 1.

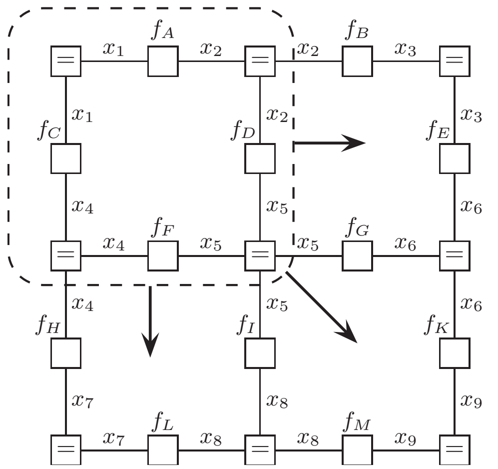

Fig. 2. Basic region of size 2×2 for a 2-D $(1, \infty)$-RLL constraint.

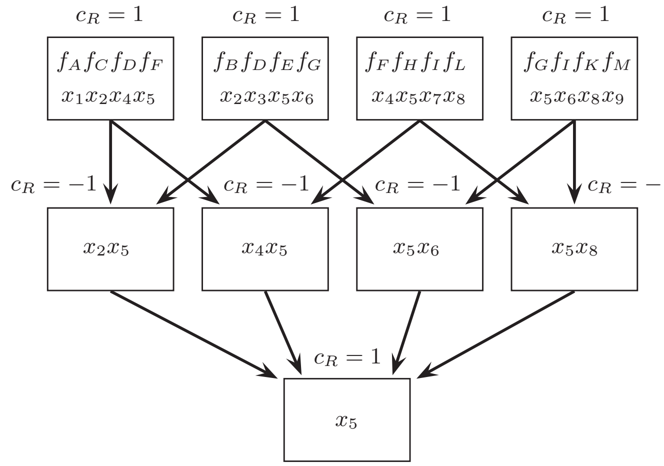

Fig. 3. The region graph for the Forney-style factor graph in Fig. 2.

In this case, the indicator function, as explained in (5), factors into a product of local kernels of the following form

$$f_a(x_i, x_j) = \begin{cases} 0, & \text{if } x_i = x_j = 1, \\ 1, & \text{otherwise,} \end{cases} \tag{8}$$

with one such factor for each adjacent pair (x_i, x_j).

The corresponding Forney-style factor graph of f is shown in Fig. 1 where the unlabeled boxes represent factors as in (8).

For this constraint, we chose basic regions with size 2×2 in a sliding window manner over the factor graph representing the factorization with local kernels as in (8), see Fig. 2.

Starting from such basic regions, we applied the cluster variation method on the factor graph in Fig. 2 to obtain the corresponding region graph depicted in Fig. 3. The counting numbers $\{c_R\}$ are shown next to each region.

In order to avoid numerical instabilities with asynchronous GBP message passing update rules, we include the factor nodes only in the basic regions. The cluster variation method counting numbers c_R ensure that each variable and factor node are counted only once. Our choice of region graph in Fig. 3 does not affect the values of the counting numbers. Moreover, since the kernels take their values in $\{0, 1\}$, considering several kernels as multiplicative factors does not affect the value of the indicator function. See [9] for more details.

IV. Numerical Experiments

Here we present the results of applying GBP to estimate the finite-sized capacity of RLL constraints.

For a 2-D RLL constraint of size $m \times m$, suppose

$$E(m) = \frac{\log_2 Z(m)}{m \times m}, \tag{9}$$

where $Z(m)$ denotes the number of 2-D binary arrays of size $m \times m$ that satisfy the constraint.

The simulation results show the convergence of E as the width of the channel m increases.

Tight upper and lower bounds were given for the Shannon capacity of a 2-D $(1, \infty)$-RLL constraint in [1]. The bounds were further improved in [15] and [8], now known to nine decimal digits.

$$0.5878911617... \leq C_{2D}^{(1,\infty)} \leq 0.5878911618...$$

For this constraint, Fig. 4 shows E defined in (9) versus the channel width over the interval $[2, 300]$. The estimation was performed using the two-way and the parent-to-child GBP algorithms. Exact values of the noiseless capacity were also computed for channels up to width $m = 6$. The horizontal line in Fig. 4 shows the Shannon capacity for this channel.

Illustrated in Fig. 5, are the numerical values for the plots in Fig. 4. For a channel of width 300, the estimated noiseless capacity is about 0.588423 which is 0.09% away from the Shannon capacity.

Shown in Fig. 6 are plots of E for 2-D $(1, \infty, d, \infty)$-RLL constraints with $d = (1, 2, 3, 4)$, versus the channel width over the interval $[2, 200]$. For a channel of width 200, the estimated noiseless capacities for $d = (2, 3, 4)$ are about $(0.499401, 0.434579, 0.386388)$. The plots are obained using the parent-to-child algorithm.

Also shown in Fig. 7 is the plot of E for a 2-D $(2, \infty)$-RLL constraint versus the channel width over the interval $[3, 400]$. Best upper and lower bounds for the Shannon capacity of a 2-D $(2, \infty)$-RLL constraint are given in [14] and [13] respectively, as

$$0.444202 \leq C_{2D}^{(2,\infty)} \leq 0.4457$$

Illustrated in Fig. 8, are the numerical values for the plots in Fig. 7. For a channel of width 400, the estimated noiseless capacity is about 0.446152 which is 0.1% away from the upper bound to the Shannon capacity [14].

Our proposed method can be generalized to compute the noiseless capacity of 3-D and higher dimensional RLL constraints. For a 3-D $(1, \infty)$-RLL constraint the following upper and lower bounds were introduced in [8] as

$$0.5225017418... \leq C_{3D}^{(1,\infty)} \leq 0.5268808478...$$

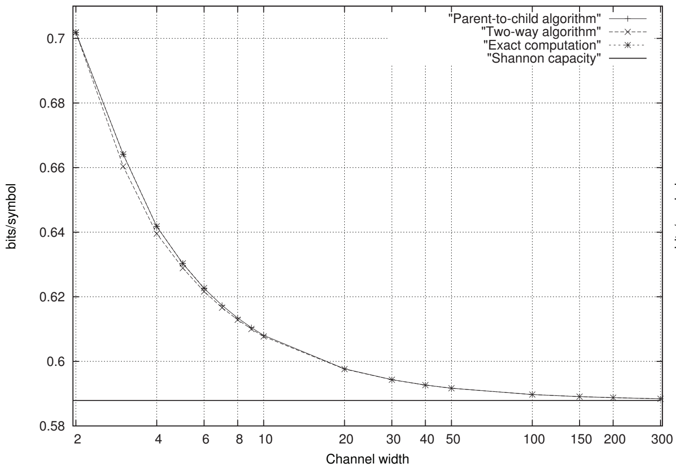

Fig. 4. Capacity estimates for a 2-D $(1, \infty)$-RLL constraint

Channel width	Parent-to-child	Two-way
2	0.701839	0.701839
4	0.641767	0.639539
6	0.622615	0.621627
8	0.613436	0.612882
10	0.608075	0.607721
20	0.597695	0.597607
30	0.594338	0.594298
40	0.592678	0.592656
50	0.591689	0.591674
100	0.589723	0.589720
150	0.589072	0.589071
200	0.588747	0.588747
300	0.588423	0.588423

Fig. 5. Numerical values for a 2-D $(1, \infty)$ channel reported in Fig. 4

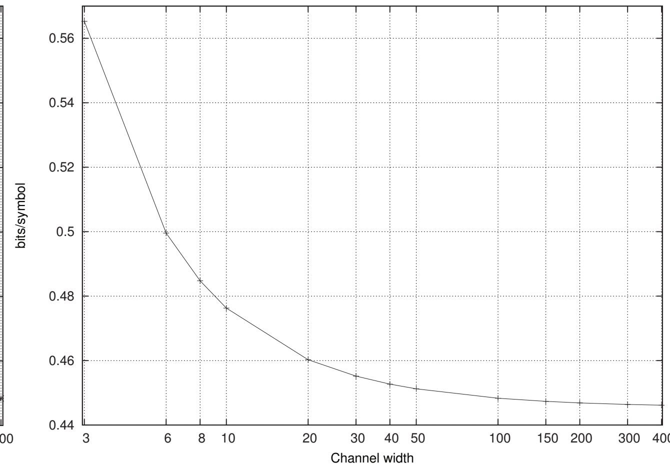

Fig. 7. Capacity estimates for a 2-D $(2, \infty)$-RLL constraint.

Channel width	Parent-to-child
3	0.565274
6	0.499583
8	0.484770
10	0.476293
20	0.460274
30	0.455197
40	0.452707
50	0.451230
100	0.448310
150	0.447347
200	0.446868
300	0.446390
400	0.446152

Fig. 8. Numerical values for a 2-D $(2, \infty)$ channel reported in Fig. 7

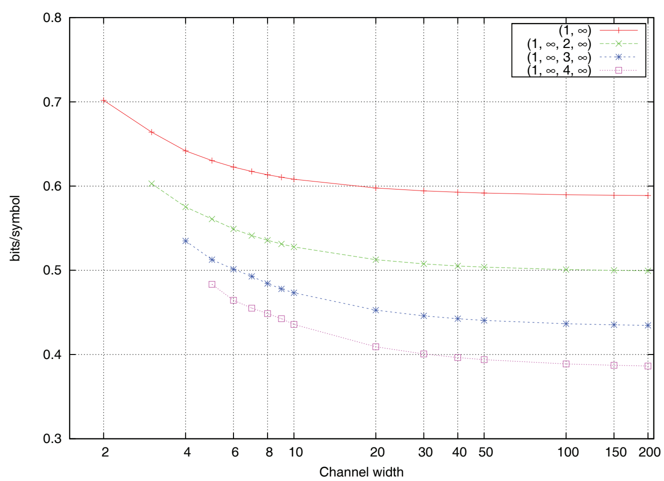

Fig. 6. Capacity estimates for a 2-D $(1, \infty, d, \infty)$-RLL constraint.

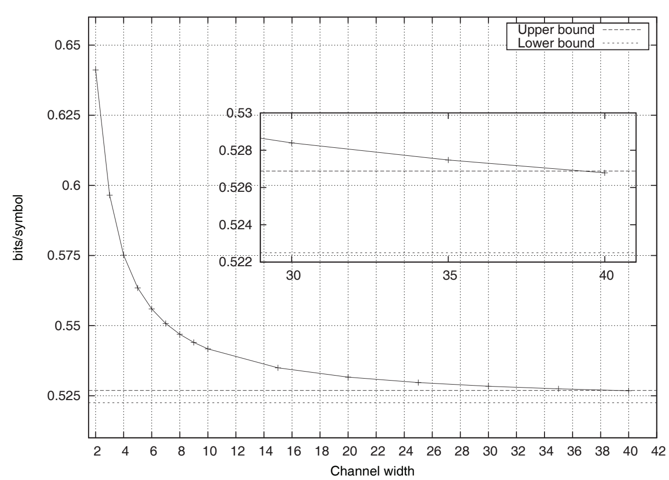

Fig. 9. Capacity estimates for a 3-D $(1, \infty)$-RLL constraint.

Fig. 9 shows the noiseless capacity estimates of a 3-D $(1, \infty)$-RLL constraint, obtained using the parent-to-child algorithm, versus the channel width m . The horizontal dotted lines show the upper and lower bounds for the Shannon capacity.

For a channel of width $m = 40$ the estimated capacity is about 0.52679 which falls within these bounds.

Simulation results and numerical values for many other constraints are reported in [9].

V. Concluding remarks

We introduced a method to estimate the noiseless capacity of two and three dimensional RLL constraints. The proposed method can be used to estimate the finite-sized noiseless capacity and to illustrate convergence to the Shannon capacity of constrained channels specially in the cases that these values are not known to a useful accuracy.

Acknowledgements

The authors gratefully acknowledge the support of Prof. H.-A. Loeliger. The first author wishes to thank Ori Shental for his helpful comments on GBP implementation.

References

[1] N.J. Calkin and H.S. Wilf, ‘The number of independent sets in a grid graph,” *SIAM J. Discr. Math.,* vol. 11, pp. 54–60, Feb. 1998.

[2] S. Forchhammer and T.V. Laursen, “Entropy of bit-stuffing-induced measures for two-dimensional checkerboard constraints,” *IEEE Trans. Inform. Theory,* vol. 53, pp. 1537–1546, April 2007.

[3] Kees A. Schouhamer Immink, *Codes for mass data storage systems.* Shannon foundation publishers, 2004.

[4] H. Ito, A. Kato, Z. Nagy, and K. Zeger, ‘Zero capacity region of multidimensional run length constraints,” *The Electronic Journal of Combinatorics,* vol. 6(1), 1999.

[5] K. Kato and K. Zeger, ‘On the capacity of two-dimensional run-length constrained channels,” *IEEE Trans. Inform. Theory,* vol. 45, pp. 1527–1540, July 1999.

[6] F. R. Kschischang, B. J. Frey, and H.-A. Loeliger, “Factor graphs and the sum-product algorithm,” *IEEE Trans. Inform. Theory,* vol. 47, pp. 498–519, Feb. 2001.

[7] H.-A. Loeliger and M. Molkaraie, “Estimating the partition function of 2-D fields and the capacity of constrained noiseless 2-D channels using tree-based Gibbs sampling,” *Proc. 2009 IEEE Information Theory Workshop,* Taormina, Italy, October 11–16, pp. 228–232.

[8] Z. Nagy and K. Zeger, ‘Capacity bounds for the three-dimensional $(0, 1)$ run-length limited channels,” *IEEE Trans. Inform. Theory,* vol. 46, pp. 1030–1033, May 2000.

[9] G. Sabato, *Simulation-based techniques to study two-dimensional ISI channels and constrained systems.* Master thesis, Dept. Inform. Techn. & Electr. Eng, ETH Zurich, Switzerland, 2009.

[10] C. E. Shannon, “A mathematical theory of communications,” *Bell Sys. Tech. Journal,* vol. 27, pp. 379–423, July 1948.

[11] O. Shental, N. Shental, S. Shamai (Shitz), I. Kanter, A. J. Weiss, and Y. Weiss, “Discrete-input two-dimensional Gaussian channels with memory: estimation and information rates via graphical models and statistical mechanics,” *IEEE Trans. Inform. Theory,* vol. 54, pp. 1500–1513, April 2008.

[12] P. H. Siegel, “Information-theoretic limits of two-dimensional optical recording channels,” in *Optical Data Storage* (Proc. of SPIE, Vol. 6282, Eds. Ryuichi Katayama and Tuviah E. Schlesinger), Montreal, Quebec, Canada, April 2006.

[13] I. Tal and R. M. Roth, “Bounds on the rate of 2-D bit-stuffing encoders,” *Proc. 2008 IEEE Int. Symp. on Information Theory,* Toronto, Canada, pp. 1463–1467.

[14] I. Tal and R. M. Roth, “Concave programming upper bounds on the capacity of 2-D constraint,” *Proc. 2009 IEEE Int. Symp. on Information Theory,* Seoul, Korea, pp. 1060–1064.

[15] W. Weeks and R. E. Blahut, “The capacity and coding gain of certain checkerboard codes,” *IEEE Trans. Inform. Theory,* vol. 44, pp. 1193–1203, May 1998.

[16] J. S. Yedidia, W. T. Freeman, and Y. Weiss. “Constructing free energy approximations and generalized belief propagation algorithms,” *IEEE Trans. Inform. Theory,* vol. 51, pp. 2282–2312, July 2005.